Computer-assisted bone augmentation, implant planning and placement: An in vitro investigation

Unger, S ; Benic, G I ; Ender, A ; Pasic, P ; Hämmerle, C H F ; Stadlinger, B

DOI: https://doi.org/10.1111/clr.14098

Received: 19 January 2022 | Revised: 19 April 2023 | Accepted: 21 April 2023

DOI: 10.1111/clr.14098

ORIGINAL ARTICLE

CLINICAL ORAL IMPLANTS RESEARCH WILEY

Computer-assisted bone augmentation, implant planning and placement: An in vitro investigation

S. Unger[1] | G. I. Benic[2] | A. Ender[3] | P. Pasic[1] | C. H. F. Hämmerle[2] | B. Stadlinger[1]

[1]Clinic of Cranio-Maxillofacial and Oral Surgery, Center of Dental Medicine, University of Zurich, Zürich, Switzerland

[2]Clinic of Fixed and Removable Prosthodontics and Dental Material Science, Center of Dental Medicine, University of Zurich, Zürich, Switzerland

[3]Clinic for Preventive Dentistry, Periodontology and Cariology, Center of Dental Medicine, University of Zurich, Zürich, Switzerland

Correspondence
S. Unger, Clinic of Cranio-Maxillofacial and Oral Surgery, Center of Dental Medicine, University of Zurich, Plattenstrasse 11, 8032 Zürich, Switzerland.
Email: silvan.unger@zzm.uzh.ch

Abstract

Aim: To assess in vitro the workflow for alveolar ridge augmentation with customised 3D printed block grafts and simultaneous computer-assisted implant planning and placement.

Methods: Twenty resin mandible models with an edentulous area and horizontal ridge defect in the region 34–36 were scanned with cone beam computed tomography (CBCT). A block graft for horizontal ridge augmentation in the region 34–36 and an implant in the position 35 were digitally planned. Twenty block grafts were 3D printed out of resin and one template for guided implant placement were stereolithographically produced. The resin block grafts were positioned onto the ridge defects and stabilised with two fixation screws each. Subsequently, one implant was inserted in the position 35 through the corresponding template for guided implant placement. Optical scans of the study models together with the fixated block graft were performed prior to and after implant placement. The scans taken after block grafting were superimposed with the virtual block grafting plan through a best-fit algorithm, and the linear deviation between the planned and the achieved block positions was calculated. The precision of the block fixation was obtained by superimposing the 20 scans taken after grafting and calculating the deviation between the corresponding resin blocks. The superimposition between the scans taken after and prior to implant placement was performed to measure a possible displacement in the block position induced by guided implant placement. The (98–2%)/2 percentile value was determined as a parameter for surface deviation.

Results: The mean deviation in the position of the block graft compared to the virtual plan amounted to 0.79 ± 0.13 mm. The mean deviation between the positions of the 20 block grafts measured 0.47 ± 0.2 mm, indicating a clinically acceptable precision. Guided implant placement induced a mean shift of 0.16 ± 0.06 mm in the position of the block graft.

Conclusions: Within the limitations of this in vitro study, it can be concluded that customised block grafts fabricated through CBCT, computer-assisted design and 3D printing allow alveolar ridge augmentation with clinically acceptable predictability and reproducibility. Computer-assisted implant planning and placement can be performed

simultaneously with computer-assisted block grafting leading to clinically non-relevant dislocation of block grafts.

KEYWORDS
3D printing, bone blocks, CBCT, implant placement

1 | INTRODUCTION

Alveolar process atrophy following tooth extraction is commonly observed in the frontal and premolar area. The process results in vertical and horizontal osseous reduction, an increase in soft tissue thickness and a narrowed band of keratinised mucosa (Majzoub et al., 2019). The physiological reason for this atrophy is the periodontal ligament blending into the bone (Cardaropoli et al., 2003). Cawood et al. (1988) classified the changes of the alveolar ridge in edentulous jaws after tooth extraction in six different stages of the ridge anatomy. Class IV (knife-edge alveolar ridge), V (flat ridge) and VI (submerged ridge) require exact assessment of the bone for the planning of implant surgery (Sutton et al., 2004).

In the first 6 months after tooth loss, the clinically relevant total bone loss is approximately 2–5 mm in the vertical dimension. After 12 months, the extent of bone loss in the horizontal dimension can rise to 50% (Lekovic et al., 1997). This implies that the width of the alveolar ridge has halved in size after 1 year. The reduction can lead to an insufficient bone bed for later implantation. Furthermore, ridge resorption can lead to an unfavourable maxilla–mandibular relationship, which requires angulations of implants and angled abutments and affects the proximity of adjacent facial concavities (maxillary sinus, nasal cavity) and vital structures (mandibular nerve; Misch et al., 1992).

The classification system created by Chiapasco et al. (2018) considers alveolar bone defects as part of the planning for prosthetically driven implant rehabilitations. It ranges from class 1 (absence of bone defect) to class 4 (a combined horizontal and vertical bone defect). The higher the class, the more extensive bone augmentation is required, and the authors recommend a delayed approach to inserting implants (Chiapasco & Casentini, 2018; Stoop et al., 2019).

Autogenous cortico-cancellous block grafts are the gold standard for the augmentation of larger alveolar defects, and the technique was already described by Brånemark et al. (1975). The blocks are often harvested intraorally from the ramus or the symphysis (Nystrom et al., 2009; Payne et al., 2018; Widmark et al., 1997).

Although the autogenous bone block is an excellent approach to augmenting vital bone, the necessity of a harvesting site is a disadvantage. Increased morbidity of the harvesting site and possible graft resorption (18%–60%) of the originally augmented volume need to be considered (Chappuis et al., 2017). High resorption rates often apply to bone blocks with a high proportion of spongious bone, especially from the iliac crest (Sbordone et al., 2012).

Bone block harvesting is a time-consuming and challenging technique. Its success correlates with the skills and experience of the surgeon. After harvesting, the bone block must be manually adapted to the recipient site and fixed with screws. Any sharp edges need to be smoothed, and the gaps must be filled with particulated bone. Due to the augmented volume, tension-free soft tissue elevation and tension-free closure are mandatory. Aloy-Prosper et al. (2015) found mucosal dehiscence as one of the most common postsurgical complications.

Cone beam computed tomography (CBCT) scans and 3D reconstructions allow a presurgical evaluation of the harvesting and recipient sites. All consecutive surgical steps are surgeon related and cannot be standardised. With the option of using allogenic or synthetic bone, computer-aided design (CAD) software tools enable customised bone blocks to be placed directly on jawbones. These bone grafts can be milled using, for example, allografts. Although the WHO found the use of allografts to be a safe procedure (Hinsenkamp et al., 2012), the method is still disputed. To bypass these concerns, 3D printing of synthetic bone presents an almost unlimited source of customisable bone for transplantation. The application of individualised bone blocks would overcome disadvantages like donor site morbidity or the misfit of a transplanted bone block to the recipient site. Customised blocks would also facilitate the surgical procedure and possibly make the outcome more predictable for future prosthetic rehabilitation.

This in vitro study investigates the accuracy and precision of bone block placement in a challenging large alveolar ridge defect by using a digital workflow. An individualised block is being constructed, fixated on the defect in a previously planned position, followed by implant placement.

2 | MATERIALS AND METHODS

2.1 | Study model

A CBCT of a mandible from the database of the Center of Dental Medicine, University of Zurich, was used for this in vitro study. The mandible presented with a full dentition without any dental restoration. The DICOM file of the CBCT was processed by using a segmentation software (Brainlab, Brainlab AG), and a digital 3D reconstruction of the mandible was exported as an STL file.

An edentulous region 34–36 with a corresponding horizontal ridge defect was digitally created (exocad, Align Technology). The extent of the bone defect was designed to simulate an atrophic jaw region in need of horizontal ridge augmentation to allow implant placement.

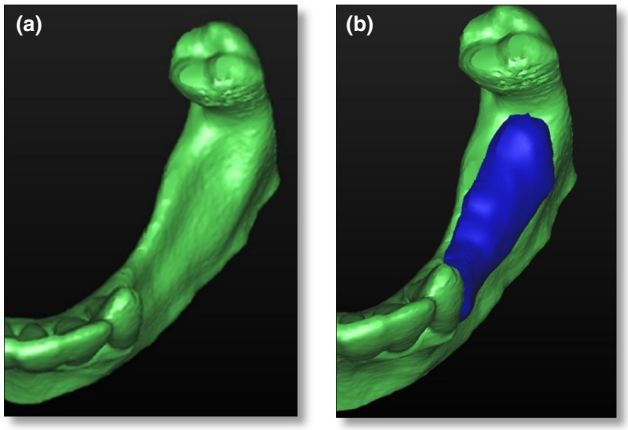

FIGURE 1 (a) The 3D reconstruction of the mandible with an edentulous area 34–36 and a horizontal ridge defect. (b) Digitally designed block graft in the edentulous area.

The jaw was 3D printed (ObjetEden 260VS Dental Advantage, Stratasys) in resin material (Objet VeroDentPlus MED690) with a 3D printing resolution of 16 µm and, subsequently, the resin model was scanned with a CBCT (3D Accuitomo, J. Morita Corp). The scan was obtained with the following technical parameters: field of view dimension 6×6 cm and voxel size of 0.125 mm (Figure 1a,b).

2.2 | Computer-assisted block graft and implant planning and placement

The DICOM file of the CBCT was imported into an implant-planning software (SimPlant, Dentsply Sirona). The software's graft volume function was used to digitally design the 3D block graft in the region 34–36.

A graft was designed to augment the horizontal ridge defect and achieve a ridge width that enables placement of 3.6-mm diameter dental implants. In its coronal portion, the block graft measured approximately 4 mm in the bucco-oral direction and 24 mm in the mesio-distal direction. Subsequently, an implant (Astra Tech OsseoSpeed EV S 3.6×8 mm, Dentsply Sirona) was virtually planned in the position 35. The digitally designed block graft was exported as an STL file. The jaw model and the block graft were 3D printed (Objet VeroDentPlus MED690, Stratasys) 20 times each in resin material (Objet VeroDentPlus MED690). One tooth-supported template for static guided placement of the implant 35 was stereolithographically fabricated by SimPlant (SimPlant; Figure 2).

One operator, experienced in bone grafting and implant placement, placed the resin block grafts and performed the guided implant placement into the 20 study models during a single session.

The 3D printed resin block graft was manually placed in the best-fitting position of the ridge defect and stabilised with two titanium fixation screws (KLS Martin, KLS Martin Group) with a length of 5 mm and a diameter of 1.5 mm. The screws were placed in the coronal part of the block in the sites 34 and 36.

One titanium implant (AstraTech Osseospeed, EV S 3.6×8 mm, Dentsply Sirona) with 3.6 mm of diameter and 8 mm of length was placed in the position 35 of each jaw model by using the prefabricated template for static guided surgery. Implant placement was performed according to the drilling protocol provided by the manufacturer. After each drilling step, the models were cleaned using water and pressurised air.

2.3 | Optical scanning and analyses

An optical surface scan of each of the 20 models with fixated resin block grafts was performed prior to and after implant placement by using an intraoral optical scanner (IOS; Sirona Primescan 2, Dentsply Sirona; Figure 3).

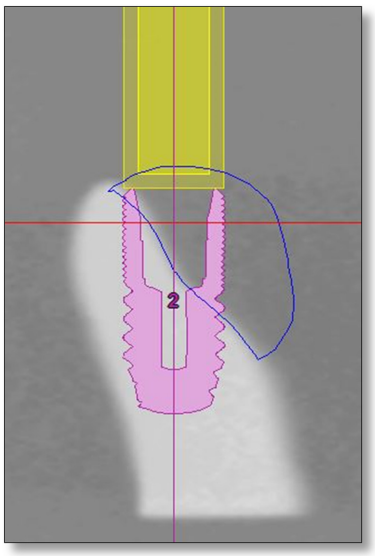

FIGURE 2 Cross-section of 3D implant and grafting planning using SimPlant software.

FIGURE 3 Jaw model after resin block fixation and guided implant placement.

The following parameters were assessed:

- accuracy and precision of grafting with 3D printed resin block
- deviation in the graft position induced through guided implant placement

The accuracy and the precision in the positioning of the block graft was assessed in comparison to the virtually planned position.

For the assessment of accuracy, the 20 optical scans of the 20 study models taken after grafting were exported as STL files. These files were superimposed with the virtual 3D plan of the graft, and the position of the block graft was compared to its initially planned position (GOM Inspect 2018/7, Carl Zeiss AG). For the superimposition of the scans after bone grafting, a best fit of the surfaces was aimed without taking into consideration the grafted region. Therefore, the area of the graft was deselected prior to the superimposition. The 3D deviation in the position of the block graft in comparison to its planned position was measured as a point-to-point signed distance in millimetre and calculated using a best-fit algorithm (GOM Inspect 2018/7, Carl Zeiss AG).

Approximately 12,000 surface point differences between the two aligned models were calculated for the calculation of the deviation (Figure 4a,b).

The same STL files from IOS taken after grafting were used for the assessment of precision. The 20 STL files were superimposed using a best-fit algorithm and the positions of the block graft were compared to each other ($n=190$) by measuring the point-to-point signed distance between the blocks (GOM Inspect 2018/7, Carl Zeiss AG).

Subsequently, the deviation of the block position induced through guided implant placement was assessed. An IOS was again performed after implant placement to create an STL file. The STL files before and the corresponding STL file after implant placement were superimposed using a best-fit algorithm ($n=20$) by measuring the point-to-point signed distance between the blocks (GOM Inspect 2018/7, Carl Zeiss AG).

2.4 | Statistical analysis

The distance measurement data between the two aligned models in millimetre was exported as CSV format and imported into a software for statistical analysis (SPSS, Version 25, IBM). The 98% and the 2% percentile were determined for each superposition and deviation measurement. The (98–2%)/2 percentile value was determined as a parameter for surface deviation. Mean, standard deviation and median values were calculated from all (98–2%)/2 percentile values (SPSS, Version 25, IBM).

3 | RESULTS

3.1 | Semi-quantitative analysis

When placed on the ridge defect within the study models, all the resin block grafts showed a good clinical fit. For visualisation purposes, all the STL files of the optical scans taken after implant placement were imported into OraCheck software (OraCheck, Generation 5, Dentsply Sirona) and superimposed with the digitally planned master file. Figure 5a,b shows the deviation of two different superimposed blocks using false colour marking. Red indicates 0.2 mm and more, blue indicates −0.2 mm and more and green indicates no deviation of the blocks. In summary, the anterior part of the blocks showed the largest deviation, followed by the posterior part. In general, the middle section was placed very precisely (Figure 5a,b).

3.2 | Accuracy of grafting with 3D printed block

The mean deviation in the position of the block graft compared to the virtual plan in the (98–2%)/2 percentile value amounted to 0.79 ± 0.13 (SD) mm. The 25% quartile reached 0.69 mm and the 75%

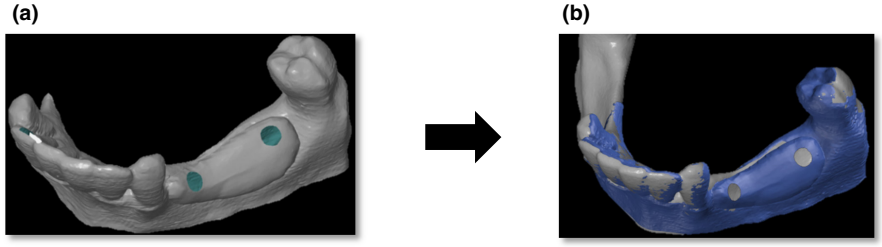

FIGURE 4 (a) STL superimposition. The cutout areas represent the screws which were excluded for to the superimposition. (b) STL superimposition. The cutout areas represent the screws which were excluded for to the superimposition.

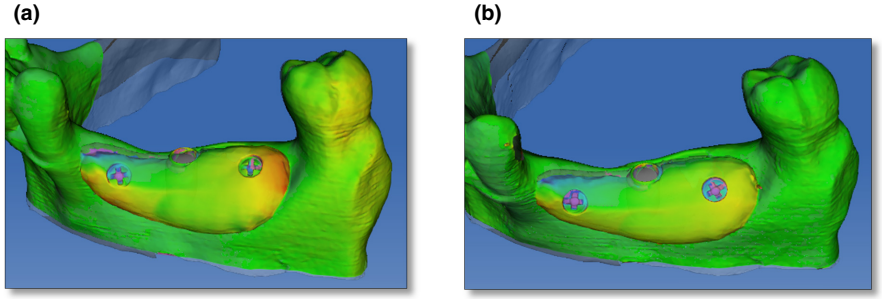

FIGURE 5 (a) Visualisation with false colour marking of the superimposition of two different block grafts (Graft 6 and Graft 8) using the OraCheck software (OraCheck, Generation 5, Dentsply Sirona). (b) Visualisation with false colour marking of the superimposition of two different block grafts (Graft 7 and Graft 8) using the OraCheck software (OraCheck, Generation 5, Dentsply Sirona).

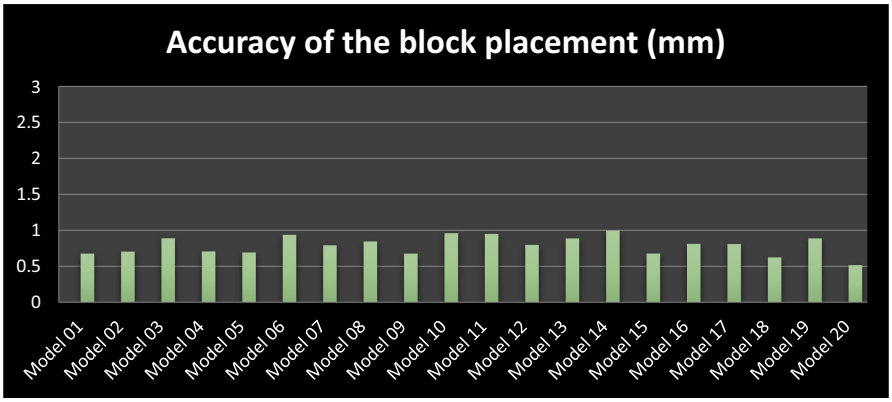

FIGURE 6 Deviation between fixated block graft and virtually planned position (percentile 98–2/2, mm).

TABLE 1 Accuracy of grafting with 3D printed block.

	Percentile (98–2%)/2
Mean (±SD)	0.79 mm (±0.13 mm)
25% quartile	0.69 mm
75% quartile	1.0 mm
Max. mean deviation	1.0 mm

quartile 1.0 mm. The maximal mean deviation of the block position in the (98–2%)/2 percentile was 1.0 mm (Figure 6; Table 1).

3.3 | Precision of grafting with 3D printed block

The mean deviation between the positions of the block grafts in the (98–2%)/2 percentile value measured 0.47 ± 0.2 (SD) mm. The 25% quartile reached was 0.32 mm and the 75% quartile was 0.58 mm. The maximal mean deviation between the block positions in the (98–2%)/2 percentile was 1.17 mm. The results show a slight trend towards increase of precision within the process of placing the blocks due to a training effect (Figure 7; Table 2).

3.4 | Deviation in the graft position induced through guided implant placement

Models 2 and 12 broke during implant placement and were excluded for this analysis. The mean (±SD) point-to-point distance between the respective surface in the (98–2%)/2 percentile value was 0.16 (±0.06) mm. The 25% quartile was 0.12 mm and the 75% quartile was 0.19 mm. The highest mean numeric deviation of the block shift after implant placement in the (98–2%)/2 percentile was 0.22 mm (Figure 8; Table 3).

4 | DISCUSSION

The aim of this study was to analyse the deviation within the placement of 3D customised printed graft blocks for alveolar ridge augmentation in vitro. Furthermore, it was ascertained whether implant placement at these augmented sites causes a shift of the fixated bone block, which to our knowledge had not been investigated previously.

The results of bone block placement in this study show a maximum numeric deviation of 1.0 mm in the 98th percentile (mean) and an overall mean of 0.79 (±0.13) mm when comparing the position of the placed block with the planned position. This presents a predictable treatment option for a comparably advanced surgical intervention. The highest deviation of the block shift post-implant placement in the 98th percentile (mean) was 0.22 mm, and the overall mean was 0.16 (±0.06) mm. These low deviation rates show that there is only minimal shifting of the block post-implant placement when using retaining screws. The in vitro figures demonstrate that mechanical stability is given even for simultaneous implant placement when retaining a block with two properly placed screws.

In contrast to the methods used in other studies, a large and smooth bone defect was artificially created (Stoop et al., 2019; Tuna et al., 2021). This method increased the difficulty of placing and retaining the block grafts. Concurring with Stoop et al. (2019), the results show that placing the customised blocks on a predefined ridge defect gives a good clinical fit. Despite the extended defect size and surface, the blocks could be comfortably positioned onto the defect at each attempt. Raghoebar et al. (2006) stated that good adaptation and fixation of the grafts to the recipient sites are important for healing. To support the complete graft integration, preparation of the recipient site is advised. The recipient site should also be perforated by multiple burr holes to enable improved vascularisation for the incorporation of a bone graft (Caneva & Botticelli, 2017). The findings support the need for precisely fitting bone blocks, especially for preserving the buccal crest. Recent in vivo studies and reviews analysed the application of CAD/CAM milled and 3D printed bone grafts and recognised their future potential, though there is currently need for additional research (Tuna et al., 2021; Yen & Stathopoulou, 2018). Stoop et al. (2019) analysed the marginal and internal fit of printed bone blocks of different sizes. They showed that a fully digital workflow using a 3D printed jaw and bone blocks of different sizes was accurate enough to meet the biological criteria for osseointegration.

Considering implant osseointegration, another aspect of this study is the one-stage approach for implant placement after block fixation. A customised block positioning avoids gaps between the

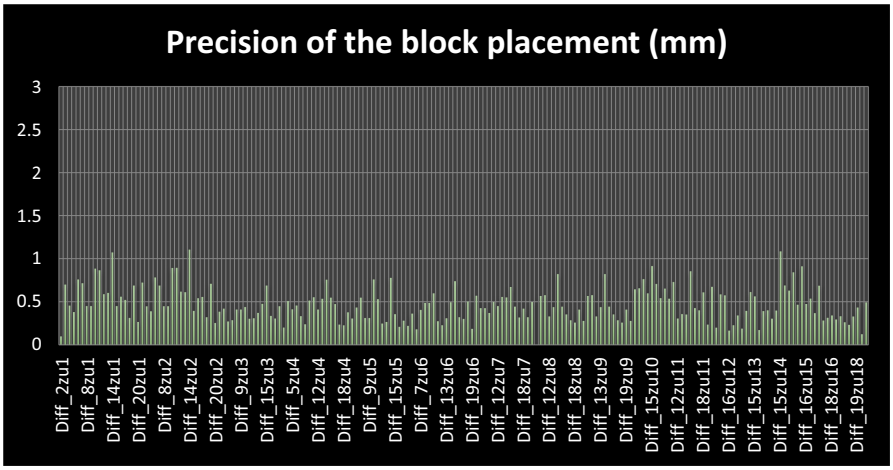

FIGURE 7 Precision of the block graft between the respective surfaces compared to each other ($n = 190$; percentile 98–2/2, mm).

TABLE 2 Precision of grafting with 3D printed block.

	Percentile (98–2%)/2
Mean (±SD)	0.47 mm (±0.2 mm)
25% quartile	0.32 mm
75% quartile	0.58 mm
Max. mean deviation	1.17 mm

block and the recipient bone. The ossification of gaps, so-called jumping gaps between an implant and the neighbouring host bone, has been intensively studied. It has been shown that a gap of less than 1 mm (Botticelli et al., 2003) can lead to sufficient bone fill without the use of grafting materials. Sanz et al. (2017) even go further and stated that there is no need for bone grafting to achieve sufficient bone filling when the jumping gap exceeds 2 mm. On the other hand, de Barros et al. (2015) showed that gaps may persist with bone formation or even the need for bone filling being necessary for proper osseointegration. The one-stage implant insertion avoids the jumping gap discussion, enabling total osseous coverage of the implant surface by the host bone and the block graft. Therefore, there is rather the question whether an implant can be osseointegrated on the vestibular side by a transplanted block graft, needing vascularisation and consecutive bone remodelling itself (Ma et al., 2021). This, however, is shown by various clinical studies, analysing the capacity of implant osseointegration following same stage bone block fixation (Michalczik & Terheyden, 2007).

Currently autologous bone blocks are considered the gold standard, particularly when large volume is required. Intraoral block grafts are mostly (Nkenke & Neukam, 2014) harvested from the mandibular ramus of the symphysis. These blocks consist primarily of cortical bone and have a limited degree of vascularisation. A bone graft with a larger share of cancellous bone can be harvested, for example, from the iliac crest. This treatment option implies hospital admission and is sometimes declined by the patient due to its invasiveness. The complications associated with harvesting the iliac crest are pain, infection, fracture of the iliac crest, scars and sensory disturbance (Joshi & Kostakis, 2004). Bone block harvesting from an intraoral donor site is less invasive (Misch, 1997), but it involves a second surgical site and the risk of necrosis of the graft and a small likelihood of nerve damage when harvesting the block.

Furthermore, proper mechanical fixation and a solid interface between the graft and the recipient site are key factors for the osseous integration of a block. De Santis et al. (2012) showed that autologous bone blocks used to augment the alveolar bony crest allow the complete osseointegration of implants after 3 months of healing. In clinics, intraorally harvested bone blocks are often difficult to adjust to the recipient site due to the discrepancy between the harvested block and the defect morphology. After positioning, the adjacent gap needs to be filled with particulated bone or bone substitute material. In addition to the difficulty of the surgical task, donor site complications are often described (Scheerlinck et al., 2013). Tumedei et al. (2019) performed a systematic review and meta-analysis comparing synthetic bone block materials with autologous blocks and empty controls in animal studies. They showed similar results when comparing synthetic blocks and autologous blocks. The synthetic blocks were superior to empty controls. Synthetic particulated bone material is already used in surgery, but we are not aware of any human studies using synthetic bone block materials.

New developments in imaging and 3D printing raise the prospect of a simpler method of augmenting large bone defects for implant placement. This study was designed to add further insights into in vivo placement of 3D printed bone grafts. A limitation of our study was the use of resin material, which mechanically differs from bone. In vivo studies in rabbits were performed using printed scaffolds to mimic autologous bone (Ghayor et al., 2020; Weber, 2019).

5 | CONCLUSIONS

Within the limitations of this in vitro study simulating the use of 3D printed block grafts for alveolar ridge augmentation in combination with guided implant placement, it can be concluded that:

- Customised block grafts fabricated through CBCT, computer-assisted design and 3D printing allow alveolar ridge augmentation with clinically acceptable predictability and reproducibility.

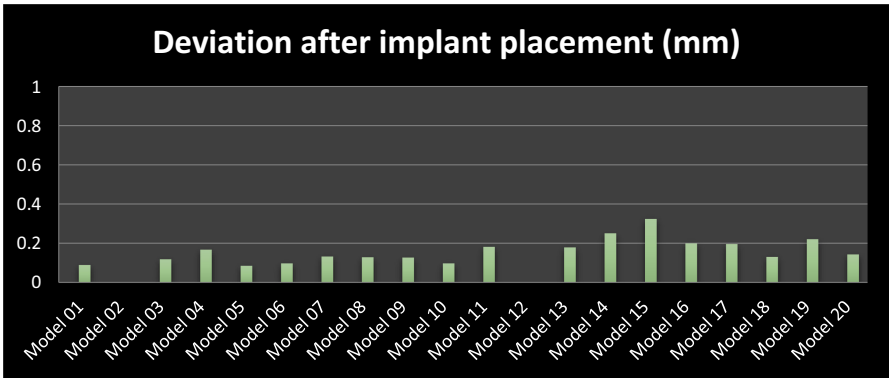

FIGURE 8 Deviation of the block grafts after implantation between the respective surfaces (percentile 98–2/2, mm).

TABLE 3 Deviation of the graft position induced through guided implant placement.

	Percentile (98–2%)/2
Mean (±SD)	0.16 mm (±0.06 mm)
25% quartile	0.12 mm
75% quartile	0.19 mm
Max. mean deviation	0.22 mm

- Computer-assisted implant planning and placement can be performed simultaneously to computer-assisted bone grafting generating minimal shifts in the position of the block graft.

AUTHOR CONTRIBUTIONS

Silvan Unger: Conceptualization (equal); data curation (lead); formal analysis (lead); investigation (lead); methodology (equal); project administration (equal); software (equal); writing – original draft (lead). **Goran Benic:** Conceptualization (equal); funding acquisition (equal); methodology (equal); supervision (equal); writing – review and editing (equal). **A. Ender:** Data curation (equal); software (equal); writing – review and editing (supporting). **Pavla Pasic:** Methodology (equal); project administration (equal). **Christoph H. F. Hämmerle:** Resources (supporting); supervision (supporting); writing – review and editing (supporting). **Bernd Stadlinger:** Conceptualization (equal); data curation (equal); funding acquisition (equal); investigation (equal); methodology (equal); resources (equal); supervision (lead); writing – review and editing (lead).

ACKNOWLEDGEMENTS

The investigators thank Tonino di Bello (Clinic of Fixed and Removable Prosthodontics and Dental Material Science, Center of Dental Medicine, University of Zurich, Switzerland) for the technical support. Open access funding provided by Universitat Zurich.

CONFLICT OF INTEREST STATEMENT

The authors report no financial interests related to any products involved in this study. This study was supported by the Clinic of Cranio-Maxillofacial and Oral Surgery and the Clinic of Fixed and Removable Prosthodontics Center of Dental Medicine, University of Zurich, Switzerland. The implants were kindly provided by DENSTPLY Implants, Germany. The fixation screws were kindly provided by KLS Martin, Tuttlingen, Germany.

ETHICAL APPROVAL

Ethics approval was not required for this in vitro study.

DATA AVAILABILITY STATEMENT

The authors confirm that the data supporting the findings of this study are available within the article.

ORCID

S. Unger https://orcid.org/0000-0002-8692-8111
G.I. Benic https://orcid.org/0000-0001-7551-7934
C. H. F. Hämmerle https://orcid.org/0000-0002-8280-7347
B. Stadlinger https://orcid.org/0000-0001-5044-7052

REFERENCES

Aloy-Prosper, A., Penarrocha-Oltra, D., Penarrocha-Diago, M., & Penarrocha-Diago, M. (2015). The outcome of intraoral onlay block bone grafts on alveolar ridge augmentations: A systematic review. *Medicina Oral, Patología Oral y Cirugía Bucal*, *20*(2), e251–e258. https://doi.org/10.4317/medoral.20194

Botticelli, D., Berglundh, T., Buser, D., & Lindhe, J. (2003). The jumping distance revisited: An experimental study in the dog. *Clinical Oral Implants Research*, *14*(1), 35–42. https://doi.org/10.1034/j.1600-0501.2003.140105.x

Brånemark, P. I., Lindström, J., Hallén, O., Breine, U., Jeppson, P. H., & Ohman, A. (1975). Reconstruction of the defective mandible. *Scandinavian Journal of Plastic and Reconstructive Surgery*, *9*(2), 116–128. https://doi.org/10.3109/02844317509022776

Caneva, M., & Botticelli, D. (2017). Healing at the interface between recipient sites and autologous block bone grafts affixed by either position or lag screw methods: A histomorphometric study in rabbits. *Clinical Oral Implants Research*, *28*(12), 1484–1491. https://doi.org/10.1111/clr.13016

Cardaropoli, G., Araújo, M., & Lindhe, J. (2003). Dynamics of bone tissue formation in tooth extraction sites. An experimental study in dogs. *Journal of Clinical Periodontology*, *30*(9), 809–818. https://doi.org/10.1034/j.1600-051x.2003.00366.x

Cawood, J. I., & Howell, R. A. (1988). A classification of the edentulous jaws. *International Journal of Oral and Maxillofacial Surgery*, *17*(4), 232–236. https://doi.org/10.1016/s0901-5027(88)80047-x

Chappuis, V., Cavusoglu, Y., Buser, D., & von Arx, T. (2017). Lateral ridge augmentation using autogenous block grafts and guided bone regeneration: A 10-year prospective case series study. *Clinical Implant Dentistry and Related Research*, *19*(1), 85–96. https://doi.org/10.1111/cid.12438

Chiapasco, M., & Casentini, P. (2018). Horizontal bone-augmentation procedures in implant dentistry: Prosthetically guided regeneration. *Periodontology 2000*, *77*(1), 213–240. https://doi.org/10.1111/prd.12219

de Barros, R. R., Novaes, A. B., Jr., Korn, P., Queiroz, A., de Almeida, A. L., Hintze, V., … Stadlinger, B. (2015). Bone formation in a local defect around dental implants coated with extracellular matrix components. *Clinical Implant Dentistry and Related Research*, *17*(4), 742–757. https://doi.org/10.1111/cid.12179

De Santis, E., Lang, N. P., Scala, A., Viganò, P., Salata, L. A., & Botticelli, D. (2012). Healing outcomes at implants installed in grafted sites: An experimental study in dogs. *Clinical Oral Implants Research*, *23*(3), 340–350. https://doi.org/10.1111/j.1600-0501.2011.02326.x

Ghayor, C., Chen, T. H., Bhattacharya, I., Özcan, M., & Weber, F. E. (2020). Microporosities in 3D-printed tricalcium-phosphate-based bone substitutes enhance osteoconduction and affect osteoclastic resorption. *International Journal of Molecular Sciences*, *21*(23), 9270. https://doi.org/10.3390/ijms21239270

Hinsenkamp, M., Muylle, L., Eastlund, T., Fehily, D., Noel, L., & Strong, D. M. (2012). Adverse reactions and events related to musculoskeletal allografts: Reviewed by the World Health Organisation project NOTIFY. *International Orthopaedics*, *36*(3), 633–641. https://doi.org/10.1007/s00264-011-1391-7

Joshi, A., & Kostakis, G. C. (2004). An investigation of post-operative morbidity following iliac crest graft harvesting. *British Dental Journal*, *196*(3), 167–171; discussion 155. https://doi.org/10.1038/sj.bdj.4810945

Lekovic, V., Kenney, E. B., Weinlaender, M., Han, T., Klokkevold, P., Nedic, M., & Orsini, M. (1997). A bone regenerative approach to alveolar ridge maintenance following tooth extraction. Report of 10 cases. *Journal of Periodontology*, *68*(6), 563–570. https://doi.org/10.1902/jop.1997.68.6.563

Ma, G., Wu, C., & Shao, M. (2021). Simultaneous implant placement with autogenous onlay bone grafts: A systematic review and meta-analysis. *International Journal of Implant Dentistry*, *7*(1), 61. https://doi.org/10.1186/s40729-021-00311-4

Majzoub, J., Ravida, A., Starch-Jensen, T., Tattan, M., & Suarez-Lopez Del Amo, F. (2019). The influence of different grafting materials on alveolar ridge preservation: A systematic review. *Journal of Oral & Maxillofacial Research*, *10*(3), e6. https://doi.org/10.5037/jomr.2019.10306

Michalczik, V., & Terheyden, H. (2007). Stabilität des Knochenniveaus an Implantaten nach Augmentation mit Unterkiefer-Blocktransplantaten.

Misch, C. (1997). Comparison of intraoral donor sites for onlay grafting prior to implant placement. *The International Journal of Oral & Maxillofacial Implants*, *12*(6), 767–776.

Misch, C. M., Misch, C. E., Resnik, R. R., & Ismail, Y. H. (1992). Reconstruction of maxillary alveolar defects with mandibular symphysis grafts for dental implants: A preliminary procedural report. *The International Journal of Oral & Maxillofacial Implants*, *7*(3), 360–366.

Nkenke, E., & Neukam, F. W. (2014). Autogenous bone harvesting and grafting in advanced jaw resorption: Morbidity, resorption and implant survival. *European Journal of Oral Implantology*, *7*(Suppl 2), S203–S217.

Nystrom, E., Nilson, H., Gunne, J., & Lundgren, S. (2009). A 9-14 year follow-up of onlay bone grafting in the atrophic maxilla. *International Journal of Oral and Maxillofacial Surgery*, *38*(2), 111–116. https://doi.org/10.1016/j.ijom.2008.10.008

Payne, A. G., Alsabeeha, N. H., Atieh, M. A., Esposito, M., Ma, S., & Anas El-Wegoud, M. (2018). Interventions for replacing missing teeth: Attachment systems for implant overdentures in edentulous jaws. *Cochrane Database of Systematic Reviews*, *10*, CD008001. https://doi.org/10.1002/14651858.CD008001.pub2

Raghoebar, G. M., Liem, R. S., Bos, R. R., van der Wal, J. E., & Vissink, A. (2006). Resorbable screws for fixation of autologous bone grafts. *Clinical Oral Implants Research*, *17*(3), 288–293. https://doi.org/10.1111/j.1600-0501.2005.01200.x

Sanz, M., Lindhe, J., Alcaraz, J., Sanz-Sanchez, I., & Cecchinato, D. (2017). The effect of placing a bone replacement graft in the gap at immediately placed implants: A randomized clinical trial. *Clinical Oral Implants Research*, *28*(8), 902–910. https://doi.org/10.1111/clr.12896

Sbordone, C., Toti, P., Guidetti, F., Califano, L., Santoro, A., & Sbordone, L. (2012). Volume changes of iliac crest autogenous bone grafts after vertical and horizontal alveolar ridge augmentation of atrophic maxillas and mandibles: A 6-year computerized tomographic follow-up. *Journal of Oral and Maxillofacial Surgery*, *70*(11), 2559–2565. https://doi.org/10.1016/j.joms.2012.07.040

Scheerlinck, L. M., Muradin, M. S., van der Bilt, A., Meijer, G. J., Koole, R., & Van Cann, E. M. (2013). Donor site complications in bone grafting: Comparison of iliac crest, calvarial, and mandibular ramus bone. *The International Journal of Oral & Maxillofacial Implants*, *28*(1), 222–227. https://doi.org/10.11607/jomi.2603

Stoop, C. C., Chatzivasileiou, K., Berkhout, W. E. R., & Wismeijer, D. (2019). Marginal and internal fit of 3D printed resin graft substitutes mimicking alveolar ridge augmentation: An in vitro pilot study. *PLoS One*, *14*(4), e0215092. https://doi.org/10.1371/journal.pone.0215092

Sutton, D. N., Lewis, B. R., Patel, M., & Cawood, J. I. (2004). Changes in facial form relative to progressive atrophy of the edentulous jaws. *International Journal of Oral and Maxillofacial Surgery*, *33*(7), 676–682. https://doi.org/10.1016/s0901-5027(03)00132-2

Tumedei, M., Savadori, P., & Del Fabbro, M. (2019). Synthetic blocks for bone regeneration: A systematic review and meta-analysis. *International Journal of Molecular Sciences*, *20*(17), 4221. https://doi.org/10.3390/ijms20174221

Tuna, T., Yilmaz, B., Hermanns-Sachweh, B., Raith, S., & Wolfart, S. (2021). From a CAD/CAM-milled, allogeneic bone block to an implant-supported fixed partial denture with angulated screw channel: A case report. *Quintessence International*, *52*(1), 56–63. https://doi.org/10.3290/j.qi.a45431

Weber, F. E. (2019). Reconsidering Osteoconduction in the era of additive manufacturing. *Tissue Engineering. Part B, Reviews*, *25*(5), 375–386. https://doi.org/10.1089/ten.TEB.2019.0047

Widmark, G., Andersson, B., & Ivanoff, C. J. (1997). Mandibular bone graft in the anterior maxilla for single-tooth implants. Presentation of surgical method. *International Journal of Oral and Maxillofacial Surgery*, *26*(2), 106–109. https://doi.org/10.1016/s0901-5027(05)80827-6

Yen, H. H., & Stathopoulou, P. G. (2018). CAD/CAM and 3D-printing applications for alveolar ridge augmentation. *Current Oral Health Reports*, *5*(2), 127–132. https://doi.org/10.1007/s40496-018-0180-4

How to cite this article: Unger, S., Benic, G., Ender, A., Pasic, P., Hämmerle, C. H. F., & Stadlinger, B. (2023). Computer-assisted bone augmentation, implant planning and placement: An in vitro investigation. *Clinical Oral Implants Research*, *34*, 719–726. https://doi.org/10.1111/clr.14098